Formation of $GdSi_2$ film on Si(111) via phase transformation assisted by interfacial SiO_2 layer

K. B. Chung, Y. K. Choi, M. H. Jang, M. Noh,[a] and C. N. Whang
Atomic-scale Surface Science Research Center and Institute of Physics and Applied Physics, Yonsei University, 134 Shinchon-dong, Sudaemoon-Ku, Seoul 120-749, Korea

H. K. Jang, E. J. Jung, and D.-H. Ko
Department of Ceramic Engineering, Yonsei University, Shinchon-dong, Sudaemoon-ku, Seoul 120-749, Korea

(Received 18 June 2004; accepted 22 November 2004; published 5 January 2005)

$GdSi_2$ film with almost perfect interface was grown on a Si(111) substrate via phase transformation assisted by interfacial SiO_2 layer. The evolution of Gd silicide and the role of an oxide layer were investigated by using *in situ* reflection of high-energy electron diffraction, x-ray diffraction (XRD), atomic force microscopy (AFM), x-ray photoelectron spectroscopy, and high-resolution transmission electron microscopy (HRTEM). The XRD and AFM results confirm structural transformation from the initial $GdSi_{1.7}$ layer to the $GdSi_2$ layer after the post-annealing at 900 °C. The HRTEM image suggests that the formation of $GdSi_2$ follows kinetic growth process, where the grain growth is dominated by the abundance of Si at the reacting surface. The thermally decomposed interfacial oxide initiates rapid phase transformation and finally results in almost perfect $GdSi_2$/Si interface without any residual oxide or mixed structure. © *2005 American Vacuum Society.* [DOI: 10.1116/1.1849222]

I. INTRODUCTION

The use of metal contacts and electrodes on the silicon-based microelectronic devices has stimulated extensive research in silicides. The formation of a silicide layer with excellent lateral uniformity is typically achieved via solid-state reaction between the deposited metal film and the Si substrate in post-annealing. For this reason, the researchers in this field have focused on the fundamental issues regarding growth kinetics, phase stability, and relationships between barrier-heights and heats of formation as well as finding materials yielding a low Schottky-barrier height.[1] The epitaxial growth of silicide film is essential to form ideal ohmic contact and Schottky barrier with stable interface.[2,3] But, it is strongly influenced by the nucleation and the growth energetics initiated at the metal-silicon interface. Previous researchers have reported many different approaches using fast beam heating,[2] a reactive capping layer,[4] and interfacial oxides[3–7] to affect the initial stage of interfacial reaction. The formation of single-phase silicide also has been an important goal since the mixed silicide phase at the interface will introduce inhomogeneity of barrier height and result in the degradation of device property.[8,9]

Among many silicides, rare-earth (RE) silicides have attracted considerable attention for the applications of infrared detectors, ohmic contacts, and interconnection in Si-based device due to their low Schottky-barrier height on *n*-type Si (less than 0.4 eV).[10–13] Moreover, their small lattice mismatch to Si(111) was suitable to lead easy epitaxial layer growth, which ensures an ideal interface structure with minimized defect states.[2,10] However, the reaction of RE metals with Si is relatively less understood compared to that of the near-noble or refractory metals.

Gd Silicide is known to be one of the most difficult ones to obtain in high quality epitaxial form among all RE silicides.[14] The two well-known crystal structures in the Gd–Si binary system are the hexagonal $GdS_{1.7}$ phase and the orthorhombic $GdSi_2$ phase. The former is formed at lower temperature with a high density of Si vacancies while the latter is formed at higher temperature. Normally, the mixed silicide phases of the $GdSi_{1.7}$ and the $GdSi_2$ result from the solid-state reaction of Gd thin films on Si substrates.[15,16] The ratio of the two different phases depends strongly on the growth conditions.[16,17] Previously, we have showed that the phase-selective synthesis of Gd-silicide film was possible.[18] In this article, we report the $GdSi_2$ layer formation with almost perfect interface through the phase transformation from the initial $GdS_{1.7}$, which occurred only at the sample prepared with an interfacial SiO_2 layer on top of Si(111) substrate. We also describe our understanding about the reaction kinetics in the formation of $GdSi_2$ film.

II. EXPERIMENTS

For this experiment, *p*-type Si(111) substrates in 20 mm $\times$ 20 mm square shape were prepared. The substrates were cleaned chemically by using the standard (RCA) method, which removed residues from the surface and resulted in the formation of a 10–20 Å thick SiO_2 layer at the substrate surface.[19,20] Then, the Si wafers were introduced into the UHV growth chamber. A Gd metal layer was deposited on the prepared Si surface via ionized beam assisted deposition from a tungsten crucible at 1×10^{-9} Torr without sample flashing. The deposition rate was maintained at 0.4 Å/s and

[a]Electronic mail: nohmk@yonsei.ac.kr

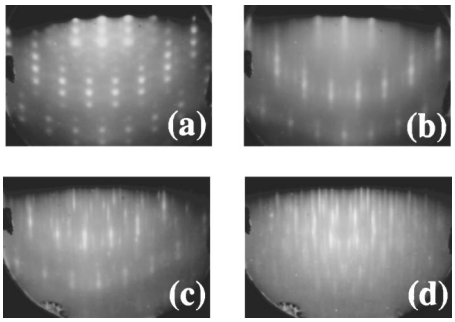

FIG. 1. RHEED patterns taken from the Gd-silicide layer grown on the oxidized Si(111) surface with the incident beam along the [112] direction after the 1 h annealing at (a) 600 °C, (b) 700 °C, (c) 800 °C, and (d) 900 °C, respectively.

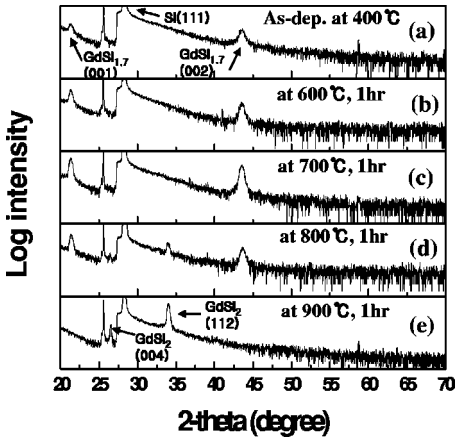

FIG. 2. XRD data collected with theta-2theta x-ray diffractometer from the samples after each indicated annealing steps.

the substrate temperature was kept at 400 °C. The 20 nm thick Gd layer was confirmed by using the Rutherford backscattering spectroscopy technique. Right after Gd deposition, the sample was annealed *in situ* under 5×10^{-10} Torr via electron bombardment. The sample temperature below 500 °C was measured by reading the applied current from the current source, where the sample temperature correspond to the current was calibrated before the experiment. Higher sample temperature was measured directly with an optical pyrometer. To examine the evolution of a Gd-silicide layer and a SiO_2 layer as a function of temperature, samples were annealed for 1 h at 600, 700, 800, and 900 °C, respectively.

The structural change of the film due to the post-annealing was monitored via *in situ* reflection of high-energy electron diffraction (RHEED). The resulted silicide phase was identified with x-ray diffraction (XRD) technique. The surface morphology of each resulting film was examined via atomic force microscopy (AFM) image. The depth profiling in x-ray photoelectron spectroscopy (XPS) was performed to release information about the chemical state and the interfacial oxide for each sample. The XPS data were collected in a Physical Electronics PHI 5700 ESCA spectrometer using Al-Kα ($h\nu$=1486.6 eV) x-ray source, with an energy resolution of 0.86 eV. The x-ray source was set at constant condition of 300 W, 15 kV, and 20 mA and the depth profiling data were collected every 30 s during the rastering of a 3 keV Ar^+ beam over sample surface. The detailed film structure and crystallinity at the interfacial region were analyzed by using high-resolution transmission electron microscopy (HRTEM).

III. RESULTS AND DISCUSSION

Figure 1 shows the RHEED patterns taken from the samples with the incident beam along the [112] direction of Si(111) substrate after the post-annealing for 1 h at (a) 600 °C, (b) 700 °C, (c) 800 °C, and (d) 900 °C, respectively. Figure 1(a) taken after the annealing at 600 °C shows hexagonal symmetry of the sample and the formation of Gd-silicide is confirmed in x-ray diffraction data. The blurred diffraction spots in Fig. 1(b) indicate the deterioration of crystallinity after the sample annealing at 700 °C. As the annealing temperature increases further, additional streaks appear on the existing pattern. The RHEED pattern representing hexagonal symmetry has completely disappeared after the sample annealing at 900 °C for 1 h as shown in Fig. 1(d). Although the change in the RHEED patterns observed above 800 °C is a clear evidence of the phase change in Gd-silicide film, it is not enough to characterize details of the accompanying structural change.

Figure 2 illustrates x-ray diffraction (XRD) data collected with theta-2theta x-ray diffractometer for the sample after each indicated annealing step. Figures 2(a)–2(e) show XRD patterns taken from the samples after (a) Gd layer deposition at 400 °C, annealing for 1 h at (b) 600 °C, (c) 700 °C, (d) 800 °C, and (e) 900 °C, respectively. These XRD patterns again clearly show the structural evolution of the Gd-silicide film. The Bragg's peaks of each XRD data were compared with those of the well-known hexagonal $GdS_{1.7}$ and the orthorhombic $GdSi_2$ phases and carefully assigned to determine the corresponding phase.[17,21] Figure 2(a) indicates that the hexagonal $GdS_{1.7}$ phase is formed after the deposition at 400 °C, as expected. The intensity of these peaks grows continuously until the annealing temperature reaches to 700 °C. At the same time, the full width half maximum (FWHM) of the (001) peak of $GdS_{1.7}$ phase was decreased to 0.5°. These results imply that the domain growth of the $GdS_{1.7}$ crystallites was continued. As the sample was annealed at 800 °C, the (112) peak of the orthorhombic $GdSi_2$ phase starts to appear and the mixed phase of $GdS_{1.7}$ and $GdSi_2$ result. In the sample annealed at 900 °C for 1 h, the hexagonal $GdS_{1.7}$ phase is completely gone and the single-phase $GdSi_2$ film with the (112) diffraction planes aligned parallel to the initial interface result. The FWHM of the (112) peak of $GdSi_2$ phase was 0.38° after annealing at 900 °C, implies better crystallinity for the $GdSi_2$ phase relative to that of the $GdS_{1.7}$ phase. XRD reveals the phase transition from the hexagonal $GdS_{1.7}$ phase to the orthorhombic $GdSi_2$ phase at temperatures above 800 °C.

The resulting samples were investigated with AFM. The surface images shown in Figs. 3(a) and 3(b) were obtained from the same samples used in XRD experiment shown in

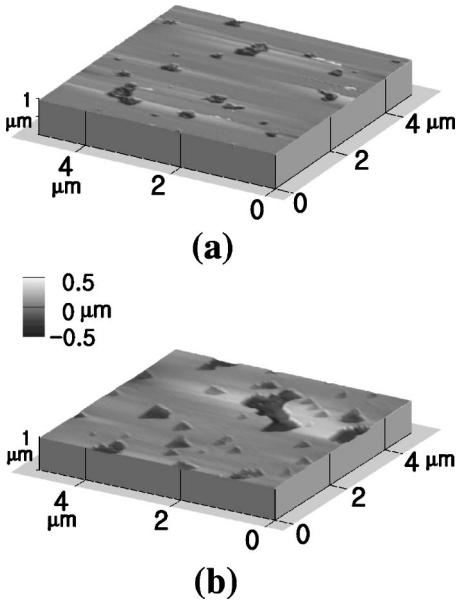

FIG. 3. AFM images collected on the samples prepared on the oxidized Si surface after the 1 h post-annealing at (a) 600 °C and (b) 900 °C, respectively.

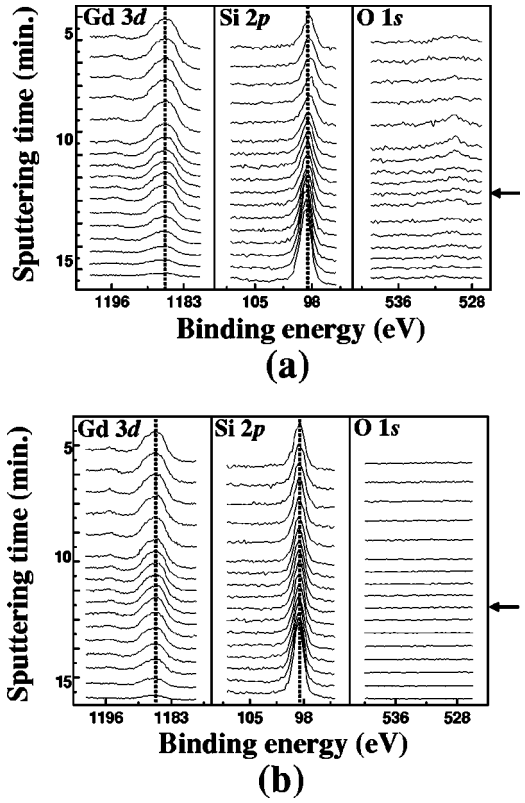

FIG. 4. XPS depth profiling spectrum taken near the interface between Gd metal and Si substrate of each samples after annealing at (a) 600 °C and (b) 900 °C, respectively.

Fig. 2. Until the annealing temperature reaches to 700 °C, the film surface gradually becomes smoother and the number of pinholes decreases. It seems due to the healing of tiny pinholes during the annealing. However, the sample surface become rougher after the sample annealing at 800 °C, which reflects the mixed phase of the hexagonal $GdS_{1.7}$ and the orthorhombic $GdSi_2$. Interestingly, surface morphology show triangular shape pinholes crystallographically aligned each other. The AFM image in Fig. 3(b) combined with the XRD pattern in Fig. 2(e) confirms single-phase layer growth of orthorhombic $GdSi_2$.

We took the Si 2*p*, O 1*s*, and Gd 3*d* core level photoemission spectra to investigate the evolution of Gd silicide and interfacial oxide as a function of annealing temperature. The surface oxides were presputtered out before the XPS data taking. Figures 4(a) and 4(b) show the XPS depth profiling data of the sample taken near the interface between Gd layer and Si substrate after annealing at 600 and 900 °C, respectively. The interface of Gd silicide and Si is estimated and indicated by an arrow based on the duration of Ar sputtering and the sputtering yield. According to the obtained Gd and Si spectra, no evidence of annealing-related chemical shifts was found near the interface area as far as the limit of XPS detection. The observation of O 1*s* signal is clear near the Si and Gd-silicide interface of the sample annealed at 600 °C, which indicates the formation of low-temperature $GdS_{1.7}$ phase directly on the top of an ultrathin interfacial oxide layer. The O 1*s* signal becomes weak as the post-annealing temperature increase and completely disappear at the sample annealed at 900 °C for 1 h. The sputtering yield is a complex function related to the sputtering rate, material density, atomic number, and incident beam conditions. In a multielement material, the lighter element is sputtered preferentially.[22] It is believed that the interfacial oxide is dissolved into gas phase SiO or O_2 and would be diffused out through the silicide layer as the annealing temperature increases.

For the detailed understanding of the oxide-layer-assisted phase transformation of the film, HRTEM images were taken. The lattice spacing in each image was calculated based on the known lattice constant of Si(111) substrate and the distribution of Gd-silicide phase was carefully assigned as represented in Fig. 5(a) as-deposited and (b) after annealing at 900 °C. As shown in Fig. 5(a), the formation of a few nanometer-size $GdSi_2$ grains are observed at the interface area while the $GdS_{1.7}$ growth with preferred crystalline orientation along (0001) direction is obvious in the as-deposited film. The nucleation of $GdSi_2$ grains seems to happen independently such that no crystallographical ordering exists between them at this stage. These results imply that the formation of $GdSi_2$ follows kinetic growth process. Remember that Si is the faster diffusing species in RE-silicide formation via solid-state reaction.[23] Thus, the $GdSi_2$ domain growth is anticipated to follow the diffusion-limited mode and dominated by the abundance of Si at the reacting interface. The growth of the Si-deficient $GdS_{1.7}$ phase is favorable initially since oxide domains act as diffusion barriers and will hinder the delivery of Si atoms from the Si substrate. As we suggested in our previous work,[18] the serious growth of $GdSi_2$ begins above the decomposition temperature of interfacial oxides. Additional supplement of Si atoms from the decomposing

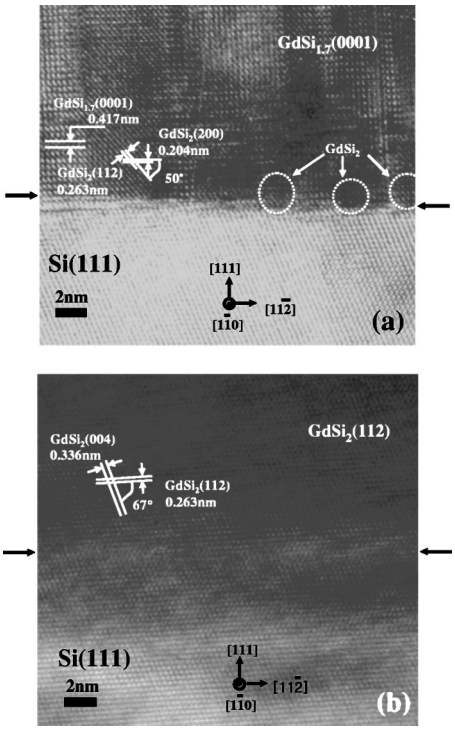

FIG. 5. HRTEM images of the samples on the oxidized Si(111) surface after (a) as-deposition at 400 °C, and (b) post-annealing at 900 °C for 1 h. The location of interface between Gd-silicide layer and Si(111) substrate is indicated by arrows in each image.

oxide at the elevated temperature facilitates $GdSi_2$ grain growth to exceed the critical size [24] that is required to continue structural transformation of Gd-silicide. HRTEM image from the sample annealed at 900 °C shows high-quality $GdSi_2$ films on Si(111) substrate. The presence of an interfacial oxide layer delivers almost perfect $GdSi_2$/Si interface without leaving any residual oxide or mixed structure shown in Fig. 5(b). The preferred orientation of the resulting $GdSi_2$ layer is assigned to (112) plane, consistent with the previous XRD and AFM results.

IV. CONCLUSION

High-quality $GdSi_2$ film with almost perfect $GdSi_2$/Si interface was grown on Si(111) substrate with the help of an interfacial oxide layer. XRD measurement revealed that the Si-deficient hexagonal $GdS_{1.7}$ phase was initially favored at low temperature and it has completely transformed to the orthorhombic $GdSi_2$ phase after the 1 h annealing at 900 °C. The crystallographically aligned triangular shape pinholes in the AFM image of the same sample confirm the epitaxial-layerlike formation of orthorhombic $GdSi_2$ film. HRTEM image implies that the growth of $GdSi_2$ follows kinetic growth process, which is dominated by the abundance of Si at the reacting surface. The serious growth of $GdSi_2$ phase begins above the decomposition temperature of interfacial oxides as the easy supplement of Si atoms become possible. The presence of an interfacial oxide layer facilitates structural transformation of Gd silicide and results in the sharp $GdSi_2$/Si interface without any residual oxide or mixed structure.

ACKNOWLEDGMENTS

This work is supported by the BK21 Project and KOSEF through the Atomic-scale Surface Science Research Center (ASSRC) at Yonsei University. Additional support by the Yonsei Center for Nano-Technology (YCNT) for M. N. is gratefully acknowledged.

[1] J. C. Phillips, in *Proceedings of the Symposium on Thin-Film Phenomena – Interfaces and Interactions*, edited by J. E. E. Baglin and J. M. Poate (Electrochemical Society, Princeton, N.J., 1978), p. 3.
[2] J. A. Knapp and S. T. Picraux, Appl. Phys. Lett. **48**, 466 (1986).
[3] R. T. Tung, Appl. Phys. Lett. **68**, 3461 (1996).
[4] C. Detavernier, R. L. Van Meirhaeghe, F. Cardon, R. A. Donaton, and K. Maek, Appl. Phys. Lett. **74**, 2930 (1999).
[5] M.-H. Cho, D.-H. Ko, Y. G. Choi, I. W. Lyo, K. Jeong, and C. N. Whang, J. Appl. Phys. **92**, 5555 (2002).
[6] J. A. Knapp, S. T. Picraux, C. S. Wu, and S. S. Lau, J. Appl. Phys. **58**, 3747 (1985).
[7] R. Hofmann, W. A. Henle, H. Öfner, M. G. Ramsey, F. P. Netzer, W. Braun, and K. Horn, Phys. Rev. B **47**, 10407 (1993).
[8] R. D. Thompson, M. Eizenberg, and K. N. Tu, J. Appl. Phys. **77**, 6763 (1981).
[9] R. D. Thompson and K. N. Tu, Thin Solid Films **93**, 265 (1982).
[10] K. N. Tu, R. D. Thompson, and B. Y. Tsuar, Appl. Phys. Lett. **38**, 626 (1981).
[11] H. Norde, J. de Sousa Pires, F. d'Heurle, F. Pesavento, S. Petersson, and P. A. Tove, Appl. Phys. Lett. **38**, 865 (1981).
[12] S. Vandré, T. Kalka, C. Preinesberger, and M. Dähne-Prietsch, Phys. Rev. Lett. **82**, 1927 (1999).
[13] R. T. Tung, Mater. Sci. Eng., R. **35**, 1 (2001).
[14] M. F. Wu, A. Vantomme, H. Pattyn, G. Langouche, and H. Bender, Appl. Phys. Lett. **68**, 3260 (1996).
[15] J. C. Chen, G. H. Shen, and L. J. Chen, Appl. Surf. Sci. **142**, 291 (1999).
[16] G. Molnár, G. Petö, E. Zsoldos, N. Q. Khánh, and Z. E. Horváth, Thin Solid Films **317**, 417 (1998).
[17] G. Molnár, I. Geröcs, G. Petö, E. Zsoldos, E. Jaráli, and J. E. Guylai, J. Appl. Phys. **64**, 6746 (1988).
[18] K. B. Chung, Y. K. Choi, M. H. Jang, M. Noh, and C. N. Whang, J. Appl. Phys. **94**, 212 (2003).
[19] W. Keren, RCA Rev. **31**, 207 (1970).
[20] W. Keren, RCA Rev. **31**, 235 (1970).
[21] G. Molnár, I. Geröcs, G. Petö, E. Zsoldos, J. Gyulai, and E. Bugiel, Appl. Phys. Lett. **58**, 249 (1991).
[22] S. Berg and I. V. Katardjiev, J. Vac. Sci. Technol. A **17**, 1916 (1999).
[23] J. E. E. Baglin, F. M. d'Heurle, and C. S. Petersson, J. Appl. Phys. **52**, 2841 (1981).
[24] A. R. West, *Solid State Chemistry and Its Applications* (Wiley, New York, 1984), p. 436.